

Benchmark experiment with iron slab by Time-of-flight technique at CIAE

Yanyan Ding¹, Yangbo Nie¹, Jie Ren¹, Xichao Ruan¹, Qi Zhao¹, Hanxiong Huang¹, Jie Bao¹, Haicheng Wu¹
¹Key Laboratory of Nuclear Data, China Institute of Atomic Energy, Beijing 102413, China

Abstract: In order to validate the evaluated nuclear data, leakage spectra in the range of 0.8 to 15 MeV from samples were measured by time-of-flight (TOF) technique using a D-T neutron source. An experimental system for benchmark validation of nuclear data with slab samples has been set up at China Institute of Atomic Energy (CIAE). In this study, test samples are iron slabs, of which the thickness are 5cm, 10cm and 15cm, and the measured angles were chosen to be about 60° and 120°. By comparing measured leakage spectrum with calculated ones by MCNP-4C code, using the data from the CENDL-3.1, ENDF/B-VIII.0, JENDL-4.0 and JEFF-3.3 nuclear data files, and the comparison was made by the spectrum shape and by the C/E values in different energy regions.

1 Introduction

The benchmark experimental study on the fusion neutronics plays an important role for validating the accuracy of the evaluated nuclear data, especially the elements that are of interests in nuclear devices, fission and fusion reactors for technologies. Fe is one of such elements that can be used as structural material of nuclear device[1]. A series of experiments on iron[2-5] have been performed to provide the experimental data base for qualifying and validating the iron nuclear data, by using the D-T neutron source or the ²⁵²Cf neutron source. However, some discrepancies between measured leakage neutron spectra and MCNP calculated ones with the different evaluated nuclear data libraries have been observed[6].

In order to validate currently available nuclear data files for iron, the leakage neutron spectra from iron slabs were measured and calculated at CIAE by using the integral benchmark facility, which has been successfully used in a series of benchmark experiments [7-10]. The leakage neutron spectra from iron slabs were measured between 0.8 MeV and 15 MeV at emission angles of 60° and 120° using TOF method with a BC501A scintillation detector. The results were compared with the calculations using a Monte Carlo code MCNP-4C[11] using the evaluated nuclear data derived from the libraries of CENDL-3.1[12], ENDF/B-VIII.0[13], JENDL-4.0[14] and JEFF-3.3[15]. The comparison was made in both the leakage neutron spectrum and the calculation-to-experiment ratio(C/E) of the spectrum integrated over four regions. Description of the experimental arrangement, the measurements, the simulations and the results will be given in the following sections.

2 Experimental procedure

The experiment was performed at CIAE, an overview of the experimental arrangement is given in Fig.1.

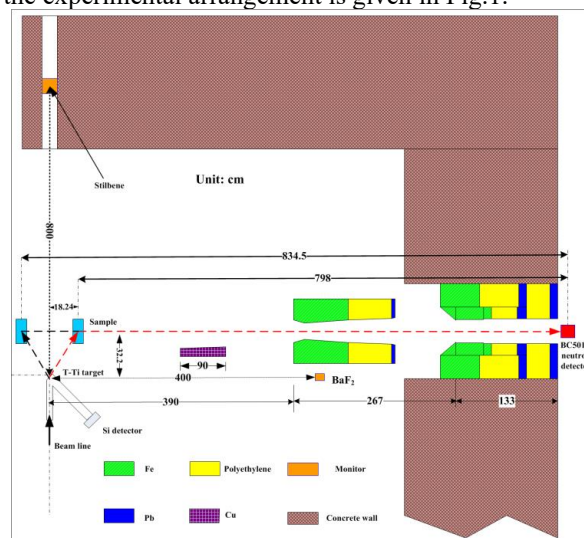


Fig. 1. Experimental arrangement for measuring the neutron leakage spectra from iron slabs.(The red dotted lines indicate the typical neutron paths)

2.1 Neutron source

An intense Deuterium-Tritium neutron source facility was used to generate neutrons. The deuteron beam which pulsed and bunched to about 2 ns width (full width at half maximum) was bombarded the tritium target to generate 14.5 MeV neutrons by the T(D, n)⁴He reactions and the repetition rate was 1.5 MHz. The number of source neutrons was estimated by alpha-particle counts

produced simultaneously in the $T(D, n)^4He$ reactions. The average neutron yield was about 1×10^9 n/s.

2.2 Iron slabs

The cylindrical plates with 13 cm in diameter and slab plates with surface area of 30 cm×30 cm were used in the present experiment, the thicknesses were chosen to be 5 cm, 10 cm and 15 cm, corresponding to 1.08, 2.16 and 3.24 mean free paths for 14.5 MeV neutrons, respectively. The chemical composition of the slabs was 99.9% iron with small amounts of impurities as shown in Table.1. The density was 7.83 g/cm³.

Table 1. The compositions of the sample(in weight).

Nuclide	Mass ratio
Fe	99.900%
Si	0.030%
C	0.015%
Mn	0.020%
Al	0.020%
Pb+Sn+Bi+Cu+S+P	0.015%

2.3 The detector and collimator

The neutron spectra leaking from slabs were detected by a BC501A liquid scintillation detector, which was located behind the concrete wall at about 8.15 m flight path in a direction perpendicular to the D+ beam line.

A stilbene scintillation crystal of 5.08 cm in diameter was placed at about 8m from the T-Ti target along with the D+ beam line for monitoring the neutron pulse shape spectra. Another BaF₂ scintillation crystal, which was located at about 4 m from the T-Ti target in a direction perpendicular to the D+ beam, was used to match the stilbene scintillation crystal to monitor the neutron source pulse shape.

In front of the neutron detector, a collimator, which was embedded inside the concrete wall of 200 cm thick with a hole of 10 cm diameter, was set to shield the neutron detector from background neutrons. A pre-collimator, which was made of iron, polyethylene and lead, was also placed between the sample and the detector to reduce the neutron background. Another 90 cm long shadow bar of Cu was also installed to eliminate the direct fast neutrons from the T-Ti source. Using such a heavy shielding and collimating system, a high foreground/background ratio has been achieved[16].

2.4 Measuring procedure and data processing

Even though the background neutrons were significantly suppressed by collimator, a background correction was necessary in the measured spectra. In order to make the background correction, two runs of measurement with sample in (foreground) and sample out (background) were performed for each sample and angle which was shown in Fig.2.

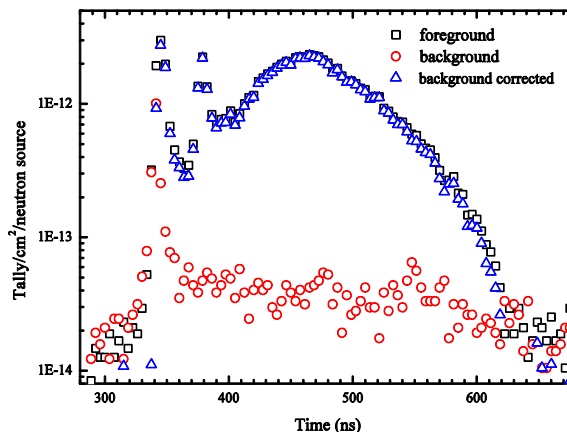


Fig.2 Experimental neutron leakage time spectra measured at 60°.

The measured angles were chosen to be nearly 60° and 120°, transformed by changing the target (sample) position along the leakage neutron direction, which results in change of the neutron emission angle from the Tritium-Titanium (T-Ti) target. As shown in Fig. 1, we put the sample on the right side of the dash line if measuring the leakage spectrum at 60°, and moved to the left side while measuring at 120°.

Polyethylene slab samples (Φ13 cm×6 cm and 30 cm×30 cm×6 cm) were used as the standard sample to calibrate the absolute neutron yield from iron samples. The leakage neutron spectrum from the polyethylene sample was measured at 60°. The comparison of the measured spectrum and the corresponding one calculated by MCNP-4C with the ENDF/B-VIII.0 evaluated nuclear data can be found in Fig.3 and Fig.4, from which it can be observed that the experimental result is well reproduced by the calculated one in the whole neutron energy range. This result indicates that the experimental apparatus and the data analysis procedures work well.

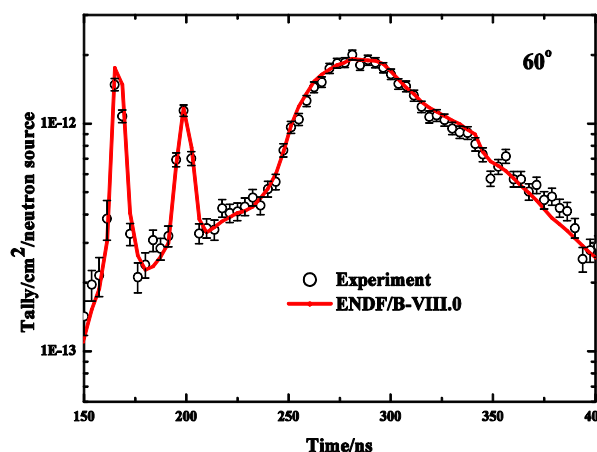


Fig.3 Leakage neutron spectrum from polyethylene sample at 60° (Φ13 cm×6 cm)

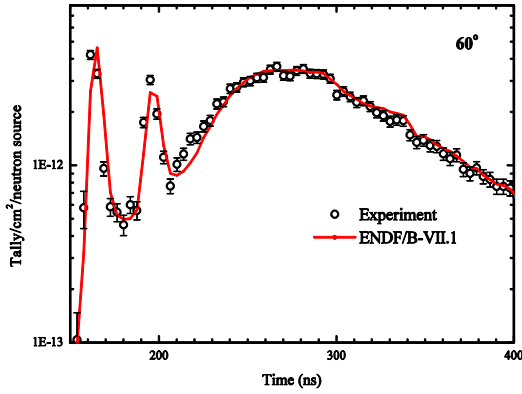


Fig.4 Leakage neutron spectrum from polyethylene sample at 60° (30 cm×30 cm×6 cm).

The uncertainties of the present experiment mainly come from the statistical and the systematic ones. The statistical uncertainty is about 5%, which includes the uncertainties of the neutrons number in per time bin (~5%), the number of n-p scattering neutrons from experiment (<0.5%) and MCNP calculation (<0.5%), respectively, the number of α particles detected for the polyethylene (<0.5%) and iron samples (<0.5%). The systematic uncertainty was mainly caused by the relative neutron detection efficiency ($\leq 3\%$) and the scattering angle ambiguity ($\leq 1\%$). Overall, the total uncertainty is less than 10%.

3. Monte Carlo simulation

For comparison of the experimental results with the calculation, the neutron leakage spectra are simulated by the MCNP-4C code using the evaluated data of iron from the CENDL-3.1, ENDF/B-VII.1, JENDL-4.0 and JEFF-3.3 libraries. In the MCNP simulation, the experimental configuration was modeled in detail, and the detailed experimental parameters were taken into account.

For sample with 13 cm in diameter the calculations for two angles of 60° and 120° were performed with the model shown in Fig. 5. Others with surface area of 30 cm×30 cm, we use the model shown in Fig. 6. Ring detector estimator (5.08cm in diameter, the same diameter as the BC501A detector) was used to tally the leakage neutron TOF spectra for comparing with the measured ones in both two models. The left sample was filled with air when the simulation was performed for 60°, while the right sample was filled with air for 120° simulation. For the background simulation, both samples were filled with air. The neutron histories adopted were 10^9 and the statistical uncertainties of each time bin were smaller than 1%.

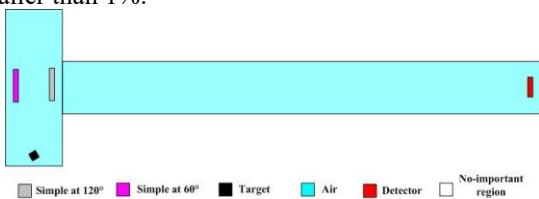


Fig.5 Model for the MCNP calculations with sample surface area of $\Phi 13$ cm.

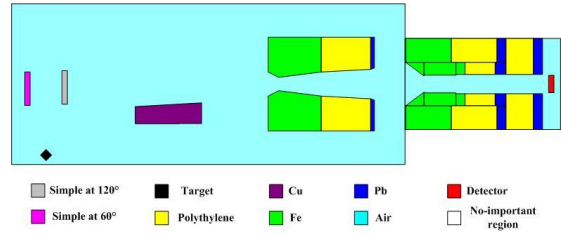


Fig.6 Model for the MCNP calculations with sample surface area of 30 cm×30 cm.

4 Results and discussion

4.1 Result of $\Phi 13$ cm

The measured leakage neutron spectra for the iron sample with 13 cm in diameter at 60° and 120° are shown in Fig. 7 comparing with the calculated ones using the four evaluated nuclear data libraries. The C/E values of the spectra integrated over specified energy ranges are also shown in Fig. 8.

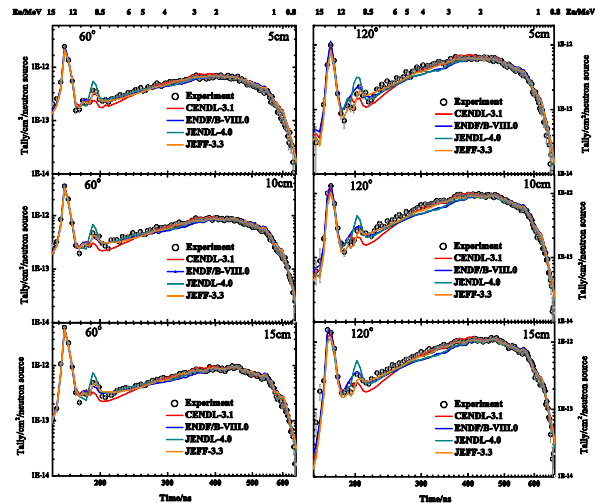


Fig.7 The comparison of measured and calculated leakage neutron spectra from iron sample ($\Phi 13$ cm) .

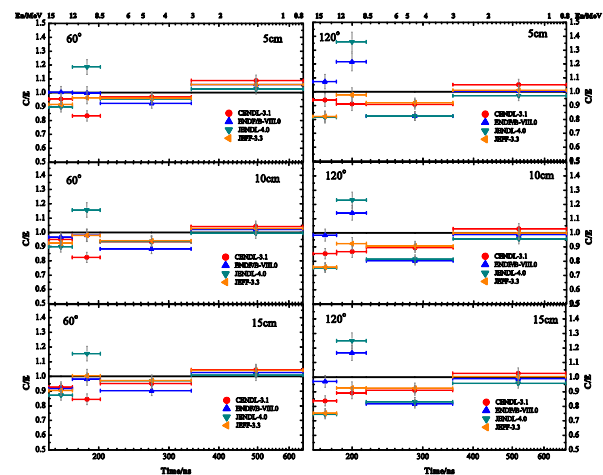


Fig.8 The C/E values integrated over the specified energy ranges at 60° ($\Phi 13$ cm) .

4.2 Result of 30 cm×30 cm

For iron sample with surface area of 30 cm×30 cm, Fig.9 shows the measured and calculated neutron leakage spectra at 60° and 120°. The C/E values of the spectra integrated over specified energy ranges are also shown in Fig.10.

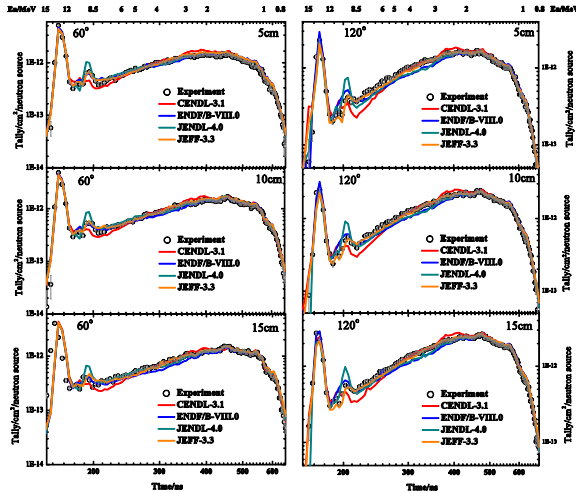


Fig.9 The comparison of measured and calculated leakage neutron spectra from iron sample (30 cm×30 cm).

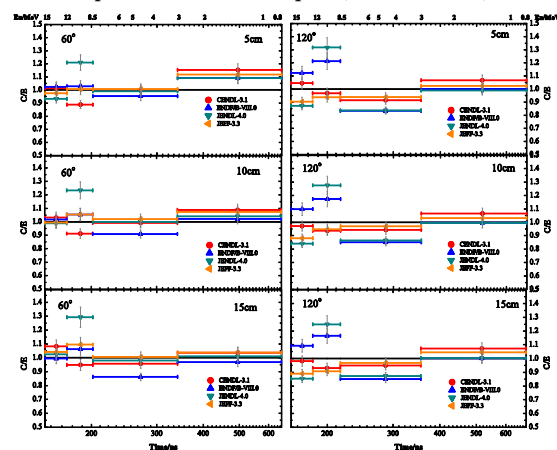


Fig.10 The C/E values integrated over the specified energy ranges at 60° (30 cm×30 cm).

From above results, we can conclude that:

(1) In the 12-15MeV range, most contribution comes from the elastic scattering. The calculated scattering peaks with the ENDF/B-VIII.0 library well reproduce the experimental ones. The calculated neutron spectra with the CENDL-3.1, JENDL-4.0 and JEFF-3.3 libraries are consistent with the experiment at 60°, but underestimated 10%-25% at 120°.

(2) In the medium energy range, 8.5-12MeV, most contribution comes from the discrete inelastic scattering. The calculated neutron spectra with the JENDL-4.0 library are overestimated around 20% at both 60° and 120°. At 60°, the results with the CENDL-3.1 library are underestimated around 15%, and at 120°, the results with the ENDF/B-VIII.0 are overestimated by more than 15%.

(3) In the 3-8.5MeV range, most contribution comes from the continuous level of inelastic scattering. The calculated neutron spectra with the CENDL-3.1 and

JEFF-3.3 libraries agree with the experiment within 11% at both 60° and 120°, while the results with the ENDF/B-VIII.0 and JENDL-4.0 libraries are underestimated about 20% at 120°.

(4) In the 0.8-3MeV range, the calculated results from all libraries agree with the experimental ones within 10%.

4.3 Discussion

In order to find the source of these discrepancies between the calculated results and the experimental ones, the total and several partial cross sections in the evaluated nuclear data libraries are studied. The contributions of different reaction channels to the leakage neutron spectra for iron at incident neutron energy of 14.5 MeV are shown in Fig.11, it can be found that the emission neutrons mainly come from the (n, el), (n, inl), and (n, 2n) reactions, and the (n, nα) and (n, np) show minor contributions.

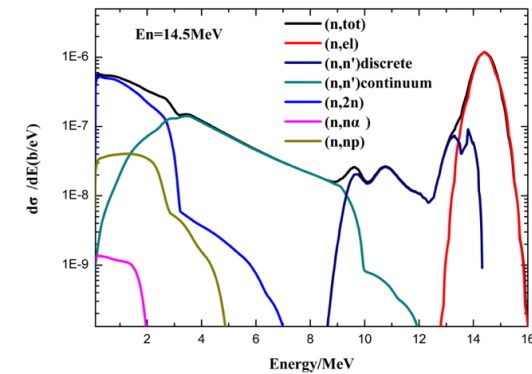


Fig.11 The distributions of leakage neutron spectra from different reactions for ^{nat}Fe (Retrieved from the CENDL-3.1 library).

The angular distributions of the neutron elastic scattering for iron are plotted in Fig.12 at the incident neutron energy of 14.5MeV, the cross sections from the ENDF/B-VIII.0 are much closer to most known experimental data than those from other libraries, especially at 60°, while the cross sections from the JENDL-4.0 and JEFF-3.3 libraries are lower than the ENDF/B-VIII.0 ones slightly at 60° and significantly at 120°, which causes the differences in the elastic scattering peak of the neutron spectra.

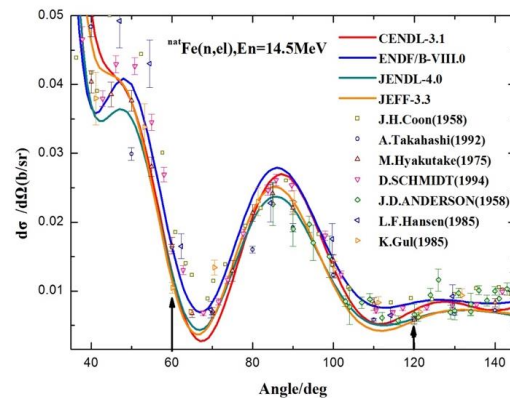


Fig.12 The angular distributions of elastic cross section for iron from different evaluated files.

The contributions from the continuum inelastic scattering at incident neutron energy of 14.5MeV are shown in Fig.13, a small, but clear peak is observed at the 8.5-11MeV range in the spectrum retrieved from the JENDL-4.0, which causes the discrepancies between the measured spectra and the calculated ones at this energy range.

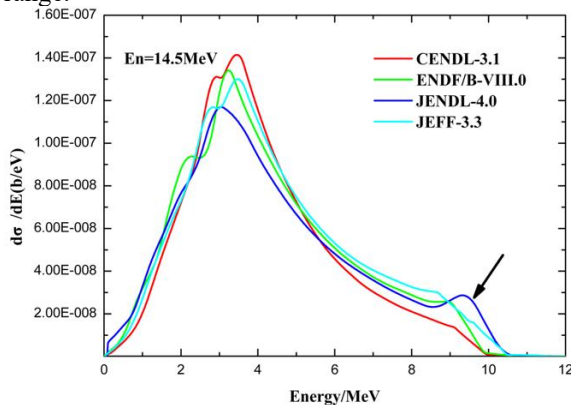


Fig.13 The contributions from the continuum inelastic scattering for iron at the incident neutron energy of 14.5 MeV

5 Summary

In this work, the validations of the evaluated nuclear data for iron were performed with two kind of samples ($\Phi 13$ cm, $30\text{ cm} \times 30\text{ cm}$), the leakage neutron spectra measured by time-of-flight method at 60° and 120° . The measured neutron energy range was 0.8-15 MeV. The theoretical calculations were carried out by MCNP-4C Monte Carlo code using the evaluated nuclear data of the CENDL-3.1, ENDF/B-VIII.0, JENDL-4.0 and JEFF-3.3 libraries. From the comparisons, it can be observed that in general the calculated neutron spectra with the CENDL-3.1 and JEFF-3.3 show better agreement with the measured ones than those with other libraries. The calculated neutron spectra with the CENDL-3.1 are underestimated slightly in the 8.5-13MeV energy range; the calculated results with the ENDF/B-VIII.0 are overestimated around 15% in the 8.5-13MeV range but underestimated about 20% in the 3-8.5MeV range at 120° ; the calculated results with the JENDL-4.0 are significantly overestimated in the 8.5-13MeV range; and the calculated results with the JENDL-4.0 and JEFF-3.3 are underestimated around 20% in the elastic scattering peak at 120° . These discrepancies originate from the improper evaluation of the angular distributions of the neutron elastic scattering and the secondary neutron energy distribution. The data in evaluated nuclear data libraries need to be improved as required in different energy ranges.

Acknowledgements

This work was supported by national nature science foundation of China (No. 11790320, 11790321, 11790323), the continuous Basic Scientific Research Project (No. WDJC-2019-09).

References

1. CHADWICK M B, DUPONT E, BAUGE E, et al. Nuclear Data Sheets. 118 (2014) 1.
2. Y. Oyama, K. Kosako, H. Maekawa, et al. Nucl. Sci. Eng. 115 (1993) 24.
3. L. F. Hansen, J. D. Anderson, P. S. Brown, et al. Nucl. Sci. Eng. 51 (1973) 278.
4. P. Bem , U. Fischer , S. Simakov, et al. Fusion Engineering and Design 69 (2003) 479.
5. B. Jansky, E. Novak, Z. Turzik, et al. Nucl. Instr. Methods Phys. Res. A 476 (2002) 358.
6. WENNER M, HAGHIGHAT A, ADAMS J M, et al. Nucl. Sci. Eng. 170 (2012) 207.
7. Yangbo Nie, Jie Bao et al. Benchmarking of evaluated nuclear data for uranium by a 14.8 MeV neutron leakage spectra experiment with slab sample[J]. Annals of Nuclear Energy, 37(2010):1456-1460.
8. R.Han, R Wada et al. Fast neutron scattering on Gallium target at 14.8 MeV[J]. Nuclear Physics A, 936(2015):17-28.
9. Y.Nie, J.Ren et al. The benchmark experiment on slab beryllium with D-T neutrons for validation of evaluated nuclear data[J]. Fusion Engineering and Design, 105(2016):8-14.
10. Zuokang Lin, Yangbo Nie et al. Benchmarking of ^{232}Th evaluation by a 14.8 MeV neutron leakage spectra experiment with slab samples[J]. Annals of Nuclear Energy, 96(2016):181-186.
11. Briesmeister. J, 2000. MCNP-A general Monte Carlo N-particle transport code system, Version 4C, Report LA 13709-M(2000) Los Alamos.
12. Z.G. Ge, Z.X. Zhao, H.H. Xia, et al. J. Korean Phys. Soc. 59 (2011) 1052.
13. D. A. Brown, M. B. Chadwick, R. Capote, et al. Nuclear Data Sheets. 148 (2018) 1.
14. K. Shibata, O. Iwamoto, T. Nakagawa et al. J. Nucl. Sci. Technol. 48 (2011) 1.
15. www.oecd-neo.org/dbdata/jeff/jeff33
16. Xinggang Cai, Yangbo Nie et al. Design of a pre-collimator system for neutronics benchmark experiment[J]. Nuclear Techniques, 2013,(01):8-13.
17. Y. Nie, J. Ren, X. Ruan, et al. Fusion Engineering and Design 105 (2016) 8.